

RESEARCH

Open Access



Potential biomarkers for predicting the overall survival outcome of kidney renal papillary cell carcinoma: an analysis of ferroptosis-related LNCRNAs

Zixuan Wu^{1,2}, Xuyan Huang², Minjie Cai^{2,3} and Peidong Huang^{1,4*}

Abstract

Background: Kidney renal papillary cell carcinoma (KIRP) is a dangerous cancer, which accounts for 15–20% of all kidney malignancies. Ferroptosis is a rare kind of cell death that overcomes medication resistance. Ferroptosis-related long non-coding RNAs (LNCRNAs) in KIRP, remain unknown.

Method: We wanted to express how ferroptosis-related LNCRNAs interact with immune cell infiltration in KIRP. Gene set enrichment analysis in the GO and KEGG databases were used to explore gene expression enrichment. The prognostic model was constructed using Lasso regression. In addition, we also analyzed the modifications in the tumor microenvironment (TME) and immunological association.

Result: The expression of LNCRNA was closely connected to the ferroptosis, according to co-expression analyses. *CASC19*, *AC090197.1*, *AC099850.3*, *AL033397.2*, *LINC00462*, and *B3GALT1-AS1* were found to be significantly increased in the high-risk group, indicating that all of these markers implicates the malignancy processes for KIRP patients and may be cancer-promoting variables. *LNCTAM34A* and *AC024022.1* were shown to be significantly elevated in the low-risk group; these might represent as the KIRP tumor suppressor genes. According to the TCGA, CCR, and inflammation-promoting genes were considered to be significantly different between the low-risk and high-risk groups. The expression of *CD160*, *TNFSF4*, *CD80*, *BTLA*, and *TNFRSF9* was different in the two risk groups.

Conclusion: LNCRNAs associated with ferroptosis were linked to the occurrence and progression of KIRP. Ferroptosis-related LNCRNAs and immune cell infiltration in the TME may be potential biomarkers in KIRP that should be further investigated.

Keywords: Kidney renal papillary cell carcinoma (KIRP), Ferroptosis-related LNCRNAs, TCGA datasets, Immune cell infiltration, Bioinformatics analysis

Introduction

Kidney cancer has become a commonly diagnosed cancer type around the world [1]. It is the second most common genitourinary system tumor in China, and the trend is increasing yearly [2]. Kidney renal papillary cell carcinoma (KIRP), which accounts for 15–20% of all kidney malignancies, arise from the proximal nephron, the same source as clear cell carcinoma [3]. However,

*Correspondence: yeruyun@163.com; huangpeidong@ynutcm.edu.cn

⁴ Second Affiliated Hospital of Yunnan University of Chinese Medicine, No. 161 Dongjiao Road, Guandu District, Kunming 650504, Yunnan Province, China

Full list of author information is available at the end of the article



in terms of disease development and patient survival outcome, KIRP is found to be a more diverse disease [4]. KIRP could be addressed in a variety of methods, including surgery, radiation, and chemotherapy, but these only provide a minor benefit [5, 6]. KIRP patients are frequently excluded from genetic studies and randomized clinical trials for kidney cancer because of the limited number of cases [7]. Yet, a lack of accurate biomarkers for early tumor detection and limited preclinical models have hampered efficient KIRP treatment therapy [8, 9]. Additional molecular identification is critical for both basic and clinical research of KIRP, in order to avoid the early onset and progression of KIRP as well as the development of novel and effective prognostic biomarkers.

LNCRNAs are a type of RNA molecules that has high levels of expression selectivity. Several studies have found that the LNCRNAs are involved in a wide range of biological activities, including gene regulation, tumor incidence, development, and metastasis regulation [10, 11]. The LNCRNAs might work together to promote the c-Myc expression and activate the Wnt signaling pathway, which is critical in developing colorectal cancer [12]. Meanwhile, the LNCRNA TUG1 was increased in hepatoblastoma, stimulating the downstream signaling pathway of JAK2/STAT3 and promoting angiogenesis in hepatoblastoma cells [13]. In non-small cell lung cancer, the LNCRNA HLA complex group 11 was demonstrated in reducing malignancy by eliminating the expression levels of carcinogenic microRNA875 [14]. However, transfection with LNCRNA short nucleolar RNA host gene eight reduced RASA1 expressions, shielding H9C2 cells against HI/R damage [15]. In recent years, ferroptosis of tumor cells has attracted a lot of attention as a new type of cell death that enables tumor cells in overcoming treatment resistance [16, 17]. Unlike apoptosis and autophagy, ferroptosis is a kind of iron-dependent and reactive oxygen species (ROS)-dependent cell death that is utilized to treat a range of disorders. Because cancer cells are more iron-dependent than normal cells and rely on it too much to proliferate, an imbalance in iron metabolism accelerates tumor growth [18]. Ferroptosis pathway activation surpasses current resistance to chemotherapeutic medications, opening up a further therapeutic frontier for cancer treatment [19]. LNCRNAs have been shown to stimulate ferroptosis regulation, control iron death, and cell apoptosis, whereas silencing the LNCRNAs considerably reduce ferroptosis and regulate inflammation and lipid peroxidation [20, 21]. Despite this, there have been rare sequence-based investigations on aberrant LNCRNA expression and its relationship with overall survival (OS) outcome of KIRP patients with iron addiction.

Immune checkpoint-related gene profiles is helpful in detecting treatment responsiveness, as well as evaluating risks and predicting survival rate of KIRP patients [22]. Despite little study has been done on the association between ferroptosis-related LNCRNAs and immune cell infiltration in KIRP, it is crucial to look into immune cell infiltration in the TME and its relationship with KIRP clinicopathological characteristics of the tumor. The causes and mechanisms of the aberrant LNCRNA expression and ferroptosis in KIRP are currently unknown. To understand the LNCRNA-related pathways that influence KIRP patients' prognosis, it is essential to construct transcriptional maps of LNCRNA expression and ferroptosis change in KIRP patients. To assess the risk and predict the overall survival outcome in KIRP patients, immune checkpoint-related gene profiles can be invoked as a predictor of therapy responsiveness. Figuring out how ferroptosis-related LNCRNAs influence the KIRP progression could lead to the discovery of a biomarker that could be exploited as a therapeutic target.

Materials and methods

We followed the methods of Yun Tang et al. 2021 [23].

Datasets and ferroptosis-related genes

The Cancer Genome Atlas was used to collect BLCA gene expression patterns and clinical data (TCGA) [24]. The expression patterns of 298 KIRP and 32 normal tissues were enrolled in the TCGA on December 3, 2021. Table 1 summarizes the clinical features of the patients. In addition, corresponding ferroptosis-related human genes were downloaded from FerrDb [25], a web-based consortium that provides a comprehensive and up-to-date

Table 1 The clinical characteristics of patients in the TCGA dataset

Variable	Number of samples
Gender	
Male/female	214/77
Age at diagnosis	
≤ 65/> 65	179/109
Grade	
G1/G2/G3/G4/NA	Unknown
Stage	
I/II/III/IV/NA	173/21/52/15/30
T	
T1/T2/T3/T4/NA	194/33/60/2/2
M	
M0/M1/NA	95/9/187
N	
N0/N1/N2/NA	50/24/4/213

database for ferroptosis markers, their regulatory molecules, and associated diseases. We identified a total of 382 ferroptosis-related genes (driver: 150; suppressor: 109; and marker: 123) (Additional file 1: Table S1a–c).

Annotation of the LNCRNAs

For annotation of the LNCRNAs in the TCGA dataset, Genome Reference Consortium Human Build 38 (GRCh38) LNCRNA annotation file was obtained from the GENCODE website⁴. Perl matched and sorted transcription data and human configuration files to acquire exact mRNA and LNCRNA data. The gene IDs were converted into gene names using the informations from the database. The R4.1.0 Limma package was used to extract ferroptosis-related gene expression data, which was based on the gene expression matrix of ferroptosis-related LNCRNA gene expression profile data that was previously collected.

Identification of the ferroptosis-related LNCRNAs

To investigate the relationship between difference ferroptosis-related LNCRNAs and KIRP, the PPI network of the target was obtained by using the String online tool [26]. Limma package's correlation test was performed to evaluate the expression of ferroptosis-related LNCRNA. Co-expression analysis was utilized to look at the relationship between ferroptosis-related gene expression and LNCRNAs. The clinical-pathology information acquired from the KIRP patients included gender, age, stage, grade, TMN, survival status, and survival time. To determine whether there was a significant difference in expression of ferroptosis-related LNCRNAs, $FDR < 0.05$ and $|\log_2FC| \geq 1$ were utilized by the limma package. First, we investigated into the function of ferroptosis-related differentially expressed genes that were both upregulated and downregulated (DEGs). The biological pathways connected with the DEGs were then analyzed using the Gene Ontology (GO). Biological processes (BP), molecular functions (MF), and cellular components (CC) regulated by the differently expressed ferroptosis-related LNCRNAs were further analyzed using a clusterProfiler, org.Hs.eg.db, enrichplot, and ggplot2 package. Based on data from the Kyoto Encyclopedia of Genes and Genomes (KEGG). In the same approach, we did a KEGG analysis on DEGs.

Development of the ferroptosis-related LNCRNAs prognostic signature

To construct a Prognostic Model, first, we grouped and merged the survival data with the LNCRNAs produced from the different analysis using the Limma package and then using the Survival package, a

ferroptosis-related LNCRNA signature was built using a Univariate Cox regression analysis. Finally, using Lasso-penalized Cox regression and Cox regression analysis stratified by risk score, a signature of ferroptosis-related LNCRNAs was created utilizing the Library Glmnet, Survival, and SurvMiner Packages (Coefficient $LNCRNA_1 \times \text{expression of } LNCRNA_1$) + (Coefficient $LNCRNA_2 \times \text{expression of } LNCRNA_2$) + ... + (Coefficient $LNCRNA_n \times \text{expression } LNCRNA_n$). Each KIRP patient's associated risk score was further evaluated. Based on the median score, the RNAs were divided into two subgroups: low- and high-risk. In Lasso regression, the low-risk (50%) and high-risk (50%) groups were identified, and the corresponding plots were obtained. The confidence interval and risk ratio were calculated after visualization, and the forest diagram was constructed. The high-risk and low-risk groups' survival curves were constructed and compared. We used the timeROC program to create a similar receiver-operating characteristics (ROC) curve to test our model's accuracy in predicting the survival outcome of KIRP patients. An independent prognosis study was carried out ensuring that our model was unaffected by other clinical prognostic variables that influences the patients' outcome. Determining the association between clinical characteristics and our prediction risk model, as well as distinguishing between the high-risk and low-risk ferroptosis-related cases. Risk and clinical correlation analyses were completed. Heatmap and limma packages were used to construct the Heatmap. To further demonstrate the correctness of our model, Decision Curve Analysis (DCA) was constructed.

Gene set enrichment analysis and the predictive nomogram

The GSEA was used to find the differences in linked functions and pathways in several samples, and data was imported using the PERL programming language. The associated score and graphs were used to determine whether or not the functions and routes in the various risk categories were dynamic. (c2.cp.kegg.v7.2.symbols.gmt, Risk.cls#h versus l). Depending on it was a high-risk cluster of prognosis-related LNCRNAs, each sample was labeled as "H" or "L". The number of permutations, no collapses, and phenotype were set to 1000. The gene list was sorted in "real" mode, with the order of the genes in "descending" mode. The "Signal2Noise" measure was utilized in ranking the genes. The normalization method was "meandiv," and the difference was statistically significant with a $FDR < 0.05$. A nomogram was constructed integrating the prognostic signatures, for predictive of 1, 2, and 3 year OS of KIRP patients.

Immunity analysis and gene expression

Simultaneously, the CIBERSORT [27, 28], ESTIMATE [29], MCPcounter [30], single-sample gene set enrichment analysis (ssGSEA) [31], and TIMER [32] algorithms were compared to evaluate cellular components or cell immune responses between the high and low risk groups based on ferroptosis-related LNCrNA signatures. First, we extracted gene expression data from the normal samples for ssGSEA analysis and adjusted the ssGSEA score. Then combined it with the risk data derived from the previous model construction. Finally, the immune function score was computed and shown using a boxplot. A heatmap was utilized to discover changes in immune response under different algorithms. In addition, ssGSEA was utilized to compare and quantify the tumor-infiltrating immune cell subgroups in both groups, as well as their immunological functions.

Statistical analysis

The data was analyzed using Bioconductor programs in R software version 4.1.0. To investigate the normally and non-normally distributed variables, the Wilcoxon test and the unpaired student's t-test were utilized. The Benjamini–Hochberg technique was used to determine the variable expressed LNCrNAs based on FDR. Utilizing "GSVA" and ssGSEA-normalized KIRP DEGs, the KIRP DEGs were compared to a genome (R-package). The sensitivity and specificity of the KIRP generates a prognostic signal in comparison with other clinicopathological factors were evaluated using the operating characteristic curve (ROC) and decision curve analysis (DCA). The connection between the ferroptosis-related LNCrNAs and clinicopathological symptoms was investigated using a logistic regression analysis and a heatmap graph. Based on the ferroptosis-related LNCrNAs signature, the Kaplan–Meier survival analysis was used to estimate the survival outcome of KIRP patients. For each analysis, statistical significance was identified as $P < 0.05$.

Results

Enrichment analysis of ferroptosis-related genes

We discovered 56 DEGs linked to ferroptosis (24 down-regulated and 32 upregulated; Additional file 1: Table S2). We obtained 427 core targets for GO analysis using the $pvalueFilter = 0.05$ and $qvalueFilter = 0.05$, including MF, CC, and BP. The MF involves oxidoreductase activity, acting on NAD(P)H (GO:0016651), oxidoreductase activity, acting on paired donors, with incorporation or reduction of molecular oxygen (GO:0016705), oxidoreductase activity, acting on the CH-OH group of donors, NAD or NADP as acceptor (GO:0016616), oxidoreductase activity, acting on CH-OH group of donors (GO:0016614). The CC mainly involves apical part of cell

(GO:0045177), NADPH oxidase complex (GO:0043020), oxidoreductase complex (GO:1990204), microvillus (GO:0005902). The BP mainly involves response to oxidative stress (GO:0006979), cellular response to oxidative stress (GO:0034599), cellular response to chemical stress (GO:0062197), response to nutrient levels (GO:0031667). In addition, the main signaling pathways were identified by KEGG enrichment analysis, revealed that the over-expressed genes were mainly involved in Chemical carcinogenesis-reactive oxygen species (hsa05208), Arachidonic acid metabolism (hsa00590), HIF-1 signaling pathway (hsa04066), Ferroptosis (hsa04216), p53 signaling pathway (hsa04115) (Fig. 1a, b and Additional file 1: Table S3a–b).

Development of a prognostic gene model and analysis of the survival outcome

945 Ferroptosis-related LNCrNAs from our Prognostic Model were discovered (Additional file 1: Table S4). 23 important LNCrNAs (LUCAT1, FOXD2-AS1, LNCTAM34A, AC130371.2, CASC19, AC090197.1, AC099850.3, AC024022.1, ITGB1-DT, DARS1-AS1, AL033397.2, LINC00462, LINC00839, FBXL19-AS1, AC096642.1, SNHG4, DUSP5-DT, AL355102.4, AL158166.1, LINC02535, SLC25A5-AS1, MNX1-AS1, B3GALT1-AS1) were discovered to be independent KIRP prognostic indicators (Fig. 2a) (Additional file 1: Table S5a). As a consequence, we calculated the risk scores for the LNCrNAs and constructed a prognostic signature. Depending on the Kaplan–Meier analyses, the expression of high-risk LNCrNA signatures were associated with poor survival outcome ($P < 0.001$, Fig. 2b). Meanwhile, the signature LNCrNAs' AUC was 1, indicating that they outperformed standard clinicopathological characteristics in predicting KIRP prognosis (Fig. 2c, d). Using a patient's risk survival status plot, we observed that the patient's risk score was inversely related to the survival of KIRP patients. Surprisingly, some of the unique LNCrNAs discovered in this work had a negative relationship with our risk model, indicated that they might be tumor suppressor genes KIRP patients. There have been few studies on them, indicating that further research is needed (Fig. 2e). The timeROC package was used to construct a comparable ROC curve to assess the accuracy of our model in predicting the survival outcomes of patients with the disease. The AUC prediction value of the unique LncRNAs signature was 1, 1, and 1, for 1, 2, and 3-year survival rates, respectively, where both areas under the curve (AUCs) were > 0.5 , attesting to our model's accuracy in predicting the disease survival outcome (Fig. 2f). The CASC19, AC090197.1, AC099850.3, AL033397.2, LINC00462, and B3GALT1-AS1 were all found to be overexpressed in the

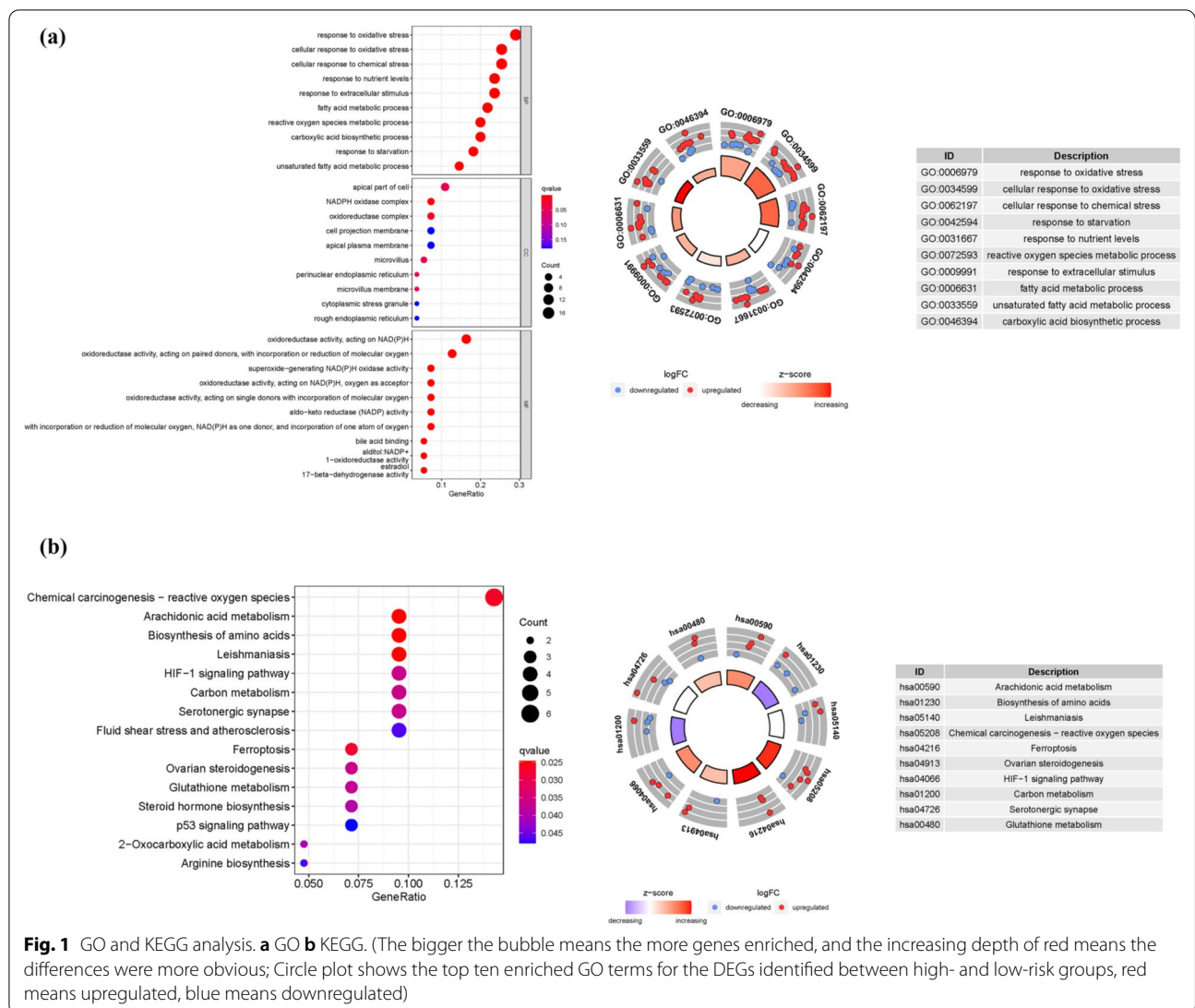
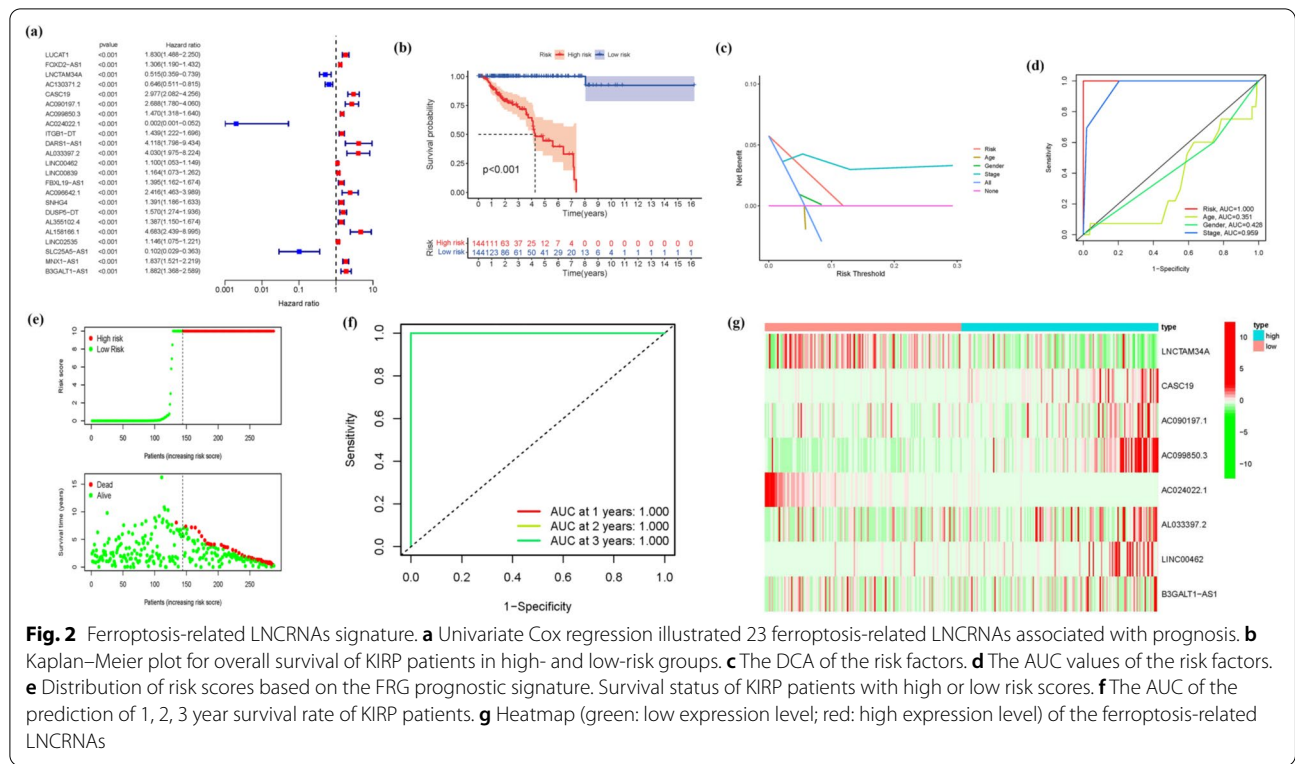


Fig. 1 GO and KEGG analysis. **a** GO **b** KEGG. (The bigger the bubble means the more genes enriched, and the increasing depth of red means the differences were more obvious; Circle plot shows the top ten enriched GO terms for the DEGs identified between high- and low-risk groups, red means upregulated, blue means downregulated)

high-risk group, suggesting that they could all be harmful to the prognosis of KIRP patients. The LNCTAM34A and AC024022.1, on the other hand, were found to be highly expressed in the low-risk group, implying that all of them could be tumor suppressor genes in KIRP patients. Because there have been few studies on these two LNCRNAs, this may be the direction of future research (Figs. 2g and Additional file 1: Table S5b). The COX analysis revealed that lncRNA signature (HR 1.280, 95CI 1.221–1.341), age (HR 1.024, 95CI 1.009–1.040), and tumor stage (HR 1.457, 95CI 1.203–1.765) were mostly independent prognostic variables for KIRP patients' OS (Fig. 3a, b). Figure 3c demonstrates the link between the LNCRNA and mRNA. Many genes were discovered to be linked to numerous LNCRNAs, and LNCRNAs were found to be associated with many genes, showing that gene and ferroptosis related LNCRNAs play diverse roles

through multi-gene crossover, which might be synergistic or antagonistic. This presents possibilities for future research. The heatmap for the prognosis signature of ferroptosis-related LNCRNAs and clinicopathological manifestations were evaluated. These eight risks LNCRNAs are not significantly associated with age or gender but are strongly connected to T, N, M, and tumor stages, with the T stage being the most significant one. This implies that the clinical professionals might use the expression of these biomarkers in KIRP patients' tumor stages as early as feasible to anticipate patients' prognoses and change of treatment regimens as needed (Fig. 3d). The hybrid nomogram (Fig. 3e), which incorporated clinicopathological features as well as the novel ferroptosis-related LNCRNAs prognostic signature, were stable and accurate, and may be used in KIRP patient care.



Gene set enrichment analysis

According to the GSEA, the majority of the new ferroptosis-related LNCRNAs prognostic signature controlled the immunological and tumor-related pathways such as DNA replication, primary immunodeficiency, ecm receptor interaction, mismatch repair, p53 signaling pathway, nod like receptor signaling pathway, etc. The top 6 enriched functions or pathways for each cluster are shown, (Fig. 4) and (Additional file 1: Table S6a–b). FDR q-value and FWER *p* value were both < 0.05. As a consequence, the “P53 SIGNALING PATHWAY” was the most enriched, and some of the genes were positively correlated with “H” or “L”.

Immunity and gene expression

Based on CIBERSORT, ESTIMATE, MCPcounter, ssGSEA, and TIMER algorithms among high and low risk groups. Figure 5a demonstrates a heatmap of immunological responses generated using the CIBERSORT, ESTIMATE, MCP counter, single-sample gene set enrichment analysis (ssGSEA), and TIMER algorithms. In addition, considering the importance of the immune system in tumor pathogenesis, the ssGSEA enrichment analysis was used in investigating the relationship between the prognostic signature risk score and immune-related function type. Figure 5b shows that the score of immune

function types, such as CCR and inflammation-promoting, were more significant in the high-risk group. However, the two immune-related functions only had one asterisk and a substantial p-value. Our findings provided essential information for tailoring treatment for KIRP patients with various risk ratings. Given the importance of checkpoint inhibitor-based immunotherapies, we looked at the changes in the immune checkpoint expression between the two groups. We identified a substantial difference in the expressions of CD160, TNFSF4, CD80, BTLA, TNFRSF9, and other genes between the two groups of patients (Fig. 5c). The expression of RBM15 was meaningful when ferroptosis-related mRNA expression was compared between the high and low risk groups (Fig. 5d). These findings suggested that RBM15 was not only involved in ferroptosis-related mRNA expression but also in the regulation of m6a, paving the way for future single-cell pan-cancer research.

Discussions

Because of its advanced stage and dismal prognosis, treating KIRP is a serious clinical challenge [33]. The molecular determination of diagnostic biomarkers especially with KIRP, should always be highlighted. According to earlier studies, ferroptosis is involved in the pathological cell death associated with degenerative disorders, and overcoming malignant cell resistance to chemotherapy

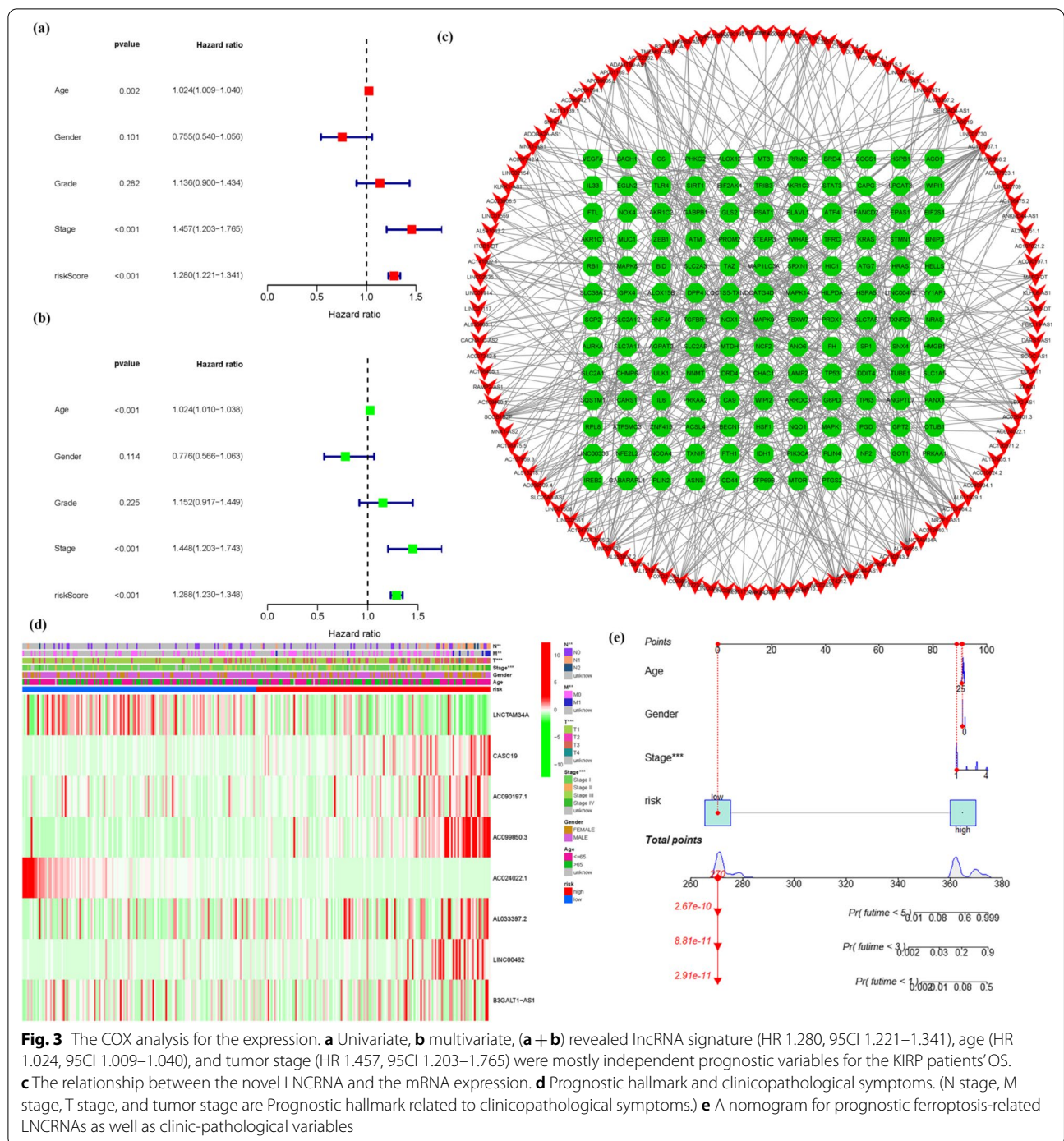


Fig. 3 The COX analysis for the expression. **a** Univariate, **b** multivariate, **(a + b)** revealed lncRNA signature (HR 1.280, 95CI 1.221–1.341), age (HR 1.024, 95CI 1.009–1.040), and tumor stage (HR 1.457, 95CI 1.203–1.765) were mostly independent prognostic variables for the KIRP patients’ OS. **c** The relationship between the novel LNCrNA and the mRNA expression. **d** Prognostic hallmark and clinicopathological symptoms. (N stage, M stage, T stage, and tumor stage are Prognostic hallmark related to clinicopathological symptoms.) **e** A nomogram for prognostic ferroptosis-related LNCrNAs as well as clinic-pathological variables

and increasing the removal of the defective cells [34, 35]. Ferroptosis offers the opportunity to act as a tumor suppressor, offering it as an alternative cancer therapy [36]. However, it is unclear how it impacts the KIRP formation through modulating the LNCrNA. This researcher investigated the role of immune infiltrating cells in the TME and immune checkpoint inhibitors in the KIRP

prognosis. The findings of this study indicated a potential biomarker and therapeutic target.

In this study, the links between the ferroptosis-related gene expression and the LNCrNAs was explored utilizing the co-expression analysis. Using the co-expression network plot, we observed a phenomenon in which numerous LNCrNAs were connected to ferroptosis-related

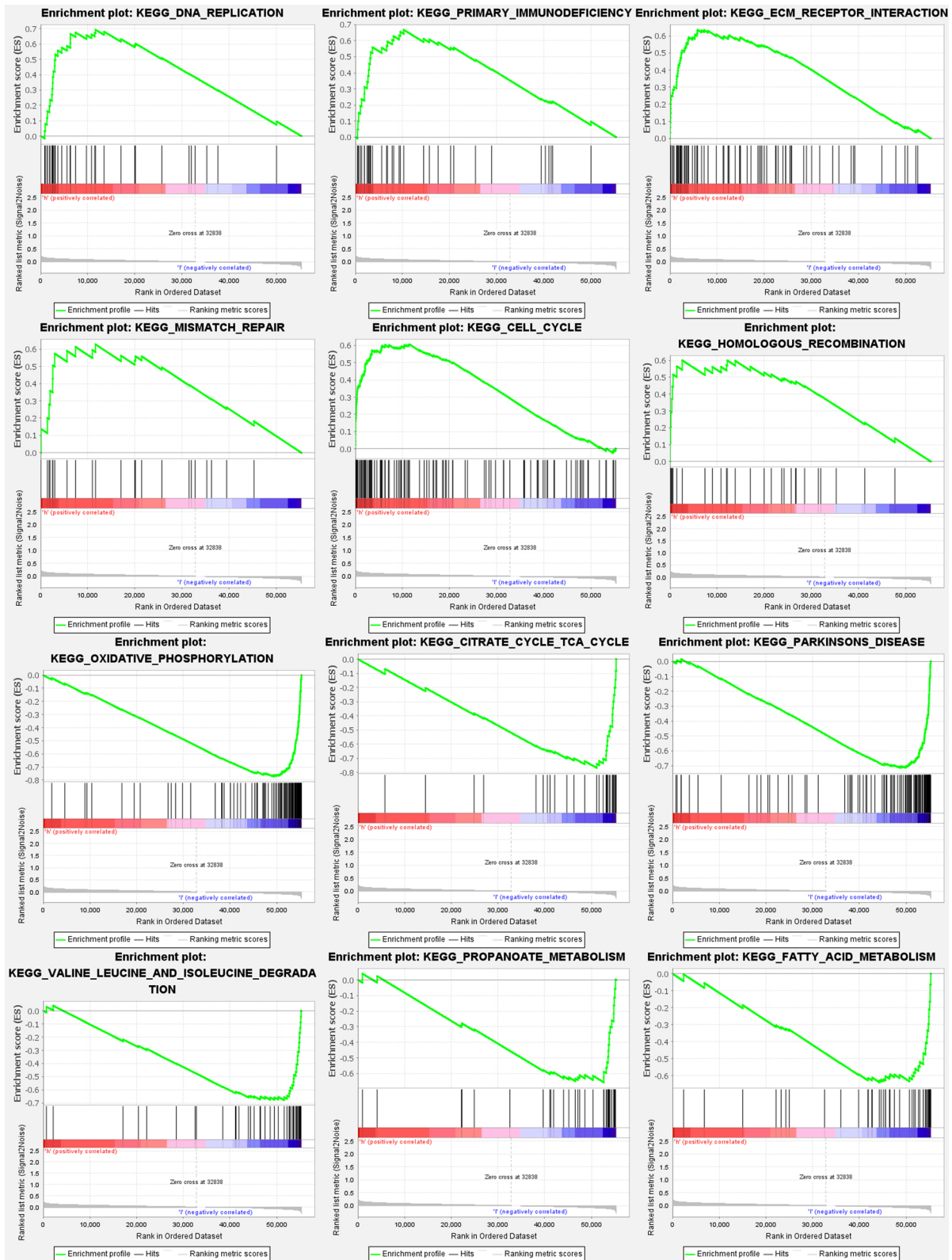


Fig. 4 Gene set enrichment analyses. To clarify the difference of related functions or pathways in different samples, the top 6 enriched functions or pathways of each cluster were listed. The most enriched pathway was the P53 signaling pathway. Both FDR q -value and FWER p value were < 0.05

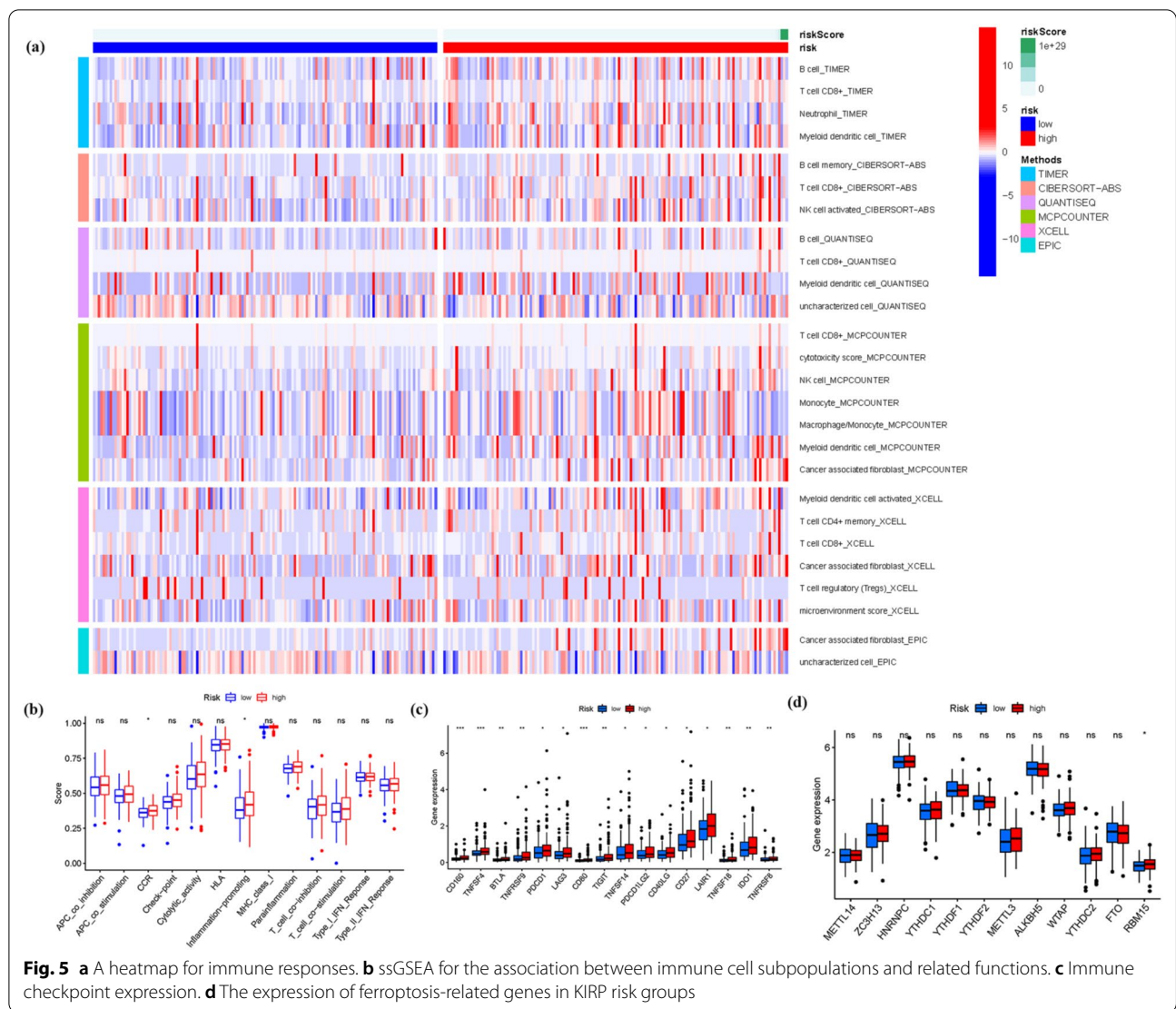


Fig. 5 **a** A heatmap for immune responses. **b** ssGSEA for the association between immune cell subpopulations and related functions. **c** Immune checkpoint expression. **d** The expression of ferroptosis-related genes in KIRP risk groups

genes in the KIRP. Following that, we discovered 56 DEGs associated with ferroptosis. The KEGG analysis further revealed that the genes participated in chemical carcinogenesis-reactive oxygen species, HIF-1 signaling pathway, ferroptosis, and p53 signaling pathway. TAZ, a Hippo pathway effector, regulates ferroptosis in the renal cell carcinoma, influencing renal cancer cell development [37]. By generating ferroptosis, ART can prevent the progression of drug-resistant kidney cancer cells [38]. In tumor organoids and patient-derived xenografts with p53 mutations or deficiencies, ferroptosis inducers (FINs) that inhibit the SLC7A11 have a strong radio sensitizing effects [39]. Ferroptosis enhanced diabetic renal tubular injury in db mice through the HIF-1 pathway visibility [40]. Ferroptosis plays a key role in KIRP.

According to the risk score, the ferroptosis-related LNCRNAs were divided into high-risk and low-risk to

investigate their probable functions in KIRP. The confidence interval and hazard ratio were identified using a data on prognosis-related LNCRNAs. Ferroptosis-related LNCRNAs appeared to be correlated with the prognosis of the KIRP in a university Cox regression study. This research discovered 8 ferroptosis-related LNCRNAs that have been connected to prognosis and have varied expression in high- and low-risk patients. Some LNCRNAs were overexpressed in high-risk individuals, while others were overexpressed in low-risk individuals ($P < 0.05$). We further investigated and examined the involvement of ferroptosis-related LNCRNAs in KIRP. Survival analysis based on the LNCRNA subtypes was used to evaluate the predictive importance of ferroptosis-related LNCRNAs. Patients with low-risk LNCRNAs had a better prognosis than those with high-risk LNCRNAs.

The CASC19, AC090197.1, AC099850.3, AL033397.2, LINC00462, and B3GALT1-AS1 were found to be upregulated in the high-risk group, indicating that all these markers were involved in the malignancy processes for KIRP sufferers and were cancer-promoting factors. The findings of the above-mentioned biomarker suggest for future work, but the concrete evidence that will be responsible for the synthesis of important transcription factors associated with ferroptosis regulation, such as Fin56, NRF2, and SFRS9 is insufficient [41–43], and is lacking, necessitating further exploration. The LNCTAM34A and AC024022.1 were found to be upregulated in the low-risk group, these genes were KIRP tumor suppressor genes.

The LncRNA AC099850.3 promotes hepatocellular carcinoma proliferation and invasion through the PRR11/PI3K/AKT axis and is associated with patients' prognosis [44]. Long non-coding RNA CASC19 facilitates non-small cell lung cancer cell proliferation and metastasis by targeting the miR-301b-3p/LDLR axis [45]. The LINC00462 promotes pancreatic cancer invasiveness through the miR-665/TGFBR1-TGFBR2/SMAD2/3 pathway [46]. According to Yujia Chen, through bioinformatics and *in vitro* experiments, demonstrated that the LNCTAM34A promotes the proliferation, migration, and epithelial-mesenchymal transition of glioma cells [47]. According to Feilong Yang, AC024022.1 is found in the cytoplasm and is a predictive biomarker in papillary renal cell cancer [48]. Since these LNCRNAs were related with the malignancy processes in KIRP sufferers, these investigations demonstrated the validity and plausibility of our results. However, little study has been conducted on LNCRNA changes associated with ferroptosis. To understand the mechanism of ferroptosis-related LNCRNA alteration and identification, more study is needed to validate our findings.

We investigated and calculated the infiltration of various immune cells in the samples to assess the role of the immune cell infiltration and the TME plays in the KIRP. Depending on a study of immune cell infiltration disparities, the CCR and inflammation-promoting factors significantly infiltrated tumor tissues in high-risk patients. As a result, these cells' invasion of the TME have a deleterious effect on the prognosis of KIRP patients. In ICI-resistant tumors, ferroptosis and immune checkpoint inhibitors (ICIs) work synergistically in boosting anticancer efficacy [49]. Only a little amount of study has been done on the link between the ICI and ferroptosis. In recent years, new ferroptosis-regulating factors have been discovered, including P53, ATF3/4, SLC7A11, ACSL4, and the BECN1 pathways. The LNCRNA is connected to the expression regulation of these factors [50], despite having little research on ferroptosis-related lncRNA and KIRP.

Based on the evidences presented above, we concluded that a change in ferroptosis-related LNCRNAs is linked to the onset and progression of KIRP.

In GSEA, the p53-signaling pathway was found to be the most enriched pathway. Several investigations have indicated that p53 has a complex role in regulating ferroptosis caused by various inducers (FINs), with a promoter and anti-ferroptosis actions depending on the setting [51–53]. Guang Lei [39] discovered that the RT-induced ferroptosis is linked to p53 activation and improved clinical outcomes in cancer patients. It is hypothesized that the ferroptosis plays a crucial role in p53-mediated radio sensitization, and that FINs should be used in conjunction with RT to treat p53 mutant malignancy. Eszter Lajkó [54] provided evidences that target the GnRH receptor serves as a successful therapeutic approach in KIRP. Depending on the GnRH isoform and the presence of 4Lys(Bu), it regulated the expressions of several apoptosis-related genes, especially the TNF, TP53, and the members of growth-factor signaling. It has a strong inhibitory effect on the expression of growth-factor signaling elements, in which the upregulation of TP53 plays an important role. Taking the aforementioned characteristics into account, ferroptosis-related LNCRNAs influence KIRP cell migration and proliferation through influencing the P53 signaling pathway. In terms of survival, the low-risk subtype outperformed the high-risk subtype. The low-risk subtype exhibited a greater survival rate than the high-risk subtype, according to the ferroptosis-related LNCRNA prognostic model. In addition, our model has a high level of accuracy in predicting KIRP patient survival rate. A rise in the risk score is associated with an increase in death rates and the high-risk ratio. Our model had no effect on other clinical prognostic factors that influence patient survival outcomes. The principle is applied to a variety of clinical situations. Based on our findings and data from the literature, ferroptosis-related LNCRNAs were viable biomarkers in predicting KIRP patient survival outcomes.

There are always constraints despite the fact that our research gives theoretical foundations and research recommendations. Our analysis has limitations, we will be unable to obtain sufficient data sources from other publicly available sites to validate the model's trustworthiness and we also limited our initial expression to the signatures of eight risk ferroptosis-related LNCRNAs, with no additional functionality or fundamental analysis.

Conclusions

In conclusion, we evaluated the expression patterns and clinical data of KIRP samples from the TCGA database to look for prognosis-related ferroptosis-related LNCRNAs. As part of the ferroptosis regulation, eight

ferroptosis-related predictive LNCRNAs were identified in 298 KIRP patients. It has significant predictive value for KIRP. Our findings added to our understanding of ferroptosis-related LNCRNAs and immune cell infiltration in the TME, opening the path for future biomarkers and prognostic indicators. It is hoped that our findings will aid in the identification of ferroptosis-related LNCRNA that drives KIRP growth, allowing us to learn more about their role in the genesis and progression of KIRP cancers.

Abbreviations

KIRP: Kidney renal papillary cell carcinoma; GO: Gene ontology; AUC: Areas under the curve; MF: Molecular functions; KEGG: Kyoto Encyclopedia of Genes and Genomes; ROC: Receiver-operating characteristics; GSEA: Gene set enrichment analyses; ICIs: Immune checkpoint inhibitors; RT: Radiotherapy; TME: Tumor microenvironment; TCGA: The Cancer Genome Atlas; LNCRNAs: Long non-coding RNAs; BP: Biological processes; CC: Cellular components; ROS: Reactive oxygen species; DCA: Decision curve analysis; FINs: Ferroptosis inducers; GnRH: Gonadotropin-releasing hormone; DEGs: Differentially expressed genes; OS: Overall survival.

Supplementary Information

The online version contains supplementary material available at <https://doi.org/10.1186/s12894-022-01037-0>.

Additional file 1. Ferroptosis-KIRC data.

Acknowledgements

Thanks to professor Huang for his strict guidance on this paper, and thanks to Miss Huang and Miss Cai for support for this paper. Thanks to reviewers and editors for their sincere comments.

Author contributions

ZW drafted and revised the manuscript. XH and MC are in charge of data collection. PH conceived and designed this article, in charge of syntax modification and revise of the manuscript. All authors read and approved the final manuscript.

Funding

National Natural Science Foundation of China Project (82160938), Exploring the mechanism of interdigitated medicine cake moxibustion against renal interstitial fibrosis from TGF- β 1-mediated interaction between ERK and Smad signaling pathway. Yunnan Provincial Health and Health Commission 2020 High-level Chinese Medicine Reserve Talents Project (Yunnan Wei Zhongming Development Development Fa [2021] No. 1). Yunnan Provincial Science and Technology Department—Chinese Medicine Joint Special Project (2019FF002-022) Exploring the mechanism study of renal interstitial fibrosis in CRF rats by spacer cake moxibustion based on the endoplasmic reticulum stress PERK signaling pathway.

Availability of data and materials

Patients who have provided informed consent for the use of their data have been included in the TCGA database, which is a public database. [TCGA] repository (<https://portal.gdc.cancer.gov/>). Users can freely obtain and publish appropriate articles based on the relevant data. Our study has no ethical difficulties or conflicts of interest because it is built on open-source data.

Declarations

Ethics approval and consent to participation

This manuscript is not a clinical trial, hence the ethics approval and consent to participation is not applicable.

Consent for publication

'Not applicable' in the consent to publish section as no human identity revealing data is used in the study.

Competing interests

The authors declare no competing financial interests.

Author details

¹Yunnan University of Chinese Medicine, Kunming 650500, Yunnan Province, China. ²Guangzhou University of Chinese Medicine, Guangzhou 510006, Guangdong Province, China. ³Shantou Health School, Shantou 515061, Guangdong Province, China. ⁴Second Affiliated Hospital of Yunnan University of Chinese Medicine, No. 161 Dongjiao Road, Guandu District, Kunming 650504, Yunnan Province, China.

Received: 22 December 2021 Accepted: 26 May 2022

Published online: 14 September 2022

References

- Znaor A, Lortet-Tieulent J, Laversanne M, Jemal A, Bray F. International variations and trends in renal cell carcinoma incidence and mortality. *Eur Urol.* 2015;67(3):519–30.
- Siegel RL, Miller KD, Fuchs HE, Jemal A. Cancer statistics, 2022. *CA Cancer J Clin.* 2022;72(1):7–33.
- Malouf GG, Su X, Zhang J, Creighton CJ, Ho TH, Lu Y, Raynal NJ, Karam JA, Tamboli P, Allanick F, et al. DNA methylation signature reveals cell ontogeny of renal cell carcinoma. *Clin Cancer Res.* 2016;22(24):6236–46.
- Linehan WM, Spellman PT, Ricketts CJ, Creighton CJ, Fei SS, Davis C, Wheeler DA, Murray BA, Schmidt L, Vocke CD, et al. Comprehensive molecular characterization of papillary renal-cell carcinoma. *N Engl J Med.* 2016;374(2):135–45.
- Tachibana H, Kondo T, Ishihara H, Fukuda H, Yoshida K, Takagi T, Izuka J, Kobayashi H, Tanabe K. Modest efficacy of nivolumab plus ipilimumab in patients with papillary renal cell carcinoma. *Jpn J Clin Oncol.* 2021;51(4):646–53.
- Chen Q, Cheng L, Li Q. The molecular characterization and therapeutic strategies of papillary renal cell carcinoma. *Expert Rev Anticancer Ther.* 2019;19(2):169–75.
- Courthod G, Tucci M, Di Maio M, Scagliotti GV. Papillary renal cell carcinoma: a review of the current therapeutic landscape. *Crit Rev Oncol Hematol.* 2015;96(1):100–12.
- Eich ML, Chau A, Mendoza RM, Guner G, Taheri D, Rodriguez PM, Sharma R, Allaf ME, Netto GJ. Tumor immune microenvironment in primary and metastatic papillary renal cell carcinoma. *Histopathology.* 2020;76(3):423–32.
- Cao H, Zhang J, Wang W. DAB2IP plays important clinical significance and correlates with immune infiltration in renal cell carcinoma. *Technol Cancer Res Treat.* 2020;19:1079204330.
- Wang R, Xing R, Su Q, Yin H, Wu D, Lv C, Yan Z. Knockdown of SFRS9 inhibits progression of colorectal cancer through triggering ferroptosis mediated by GPX4 reduction. *Front Oncol.* 2021;11:683589.
- Chaudhary N, Choudhary BS, Shah SG, Khapare N, Dwivedi N, Gaikwad A, Joshi N, Raichanna J, Basu S, Gurjar M, et al. Lipocalin 2 expression promotes tumor progression and therapy resistance by inhibiting ferroptosis in colorectal cancer. *Int J Cancer.* 2021;149(7):1495–511.
- Wang H, Zhu Y, Chen H, Yang N, Wang X, Li B, Ying P, He H, Cai Y, Zhang M, et al. Colorectal cancer risk variant rs7017386 modulates two oncogenic lncRNAs expression via ATF1-mediated long-range chromatin loop. *Cancer Lett.* 2021;518:140–51.
- Yuan MX, Ji CY, Gao HQ, Sheng XY, Xie WX, Yin Q. lncRNA TUG1 regulates angiogenesis via the miR2045p/JAK2/STAT3 axis in hepatoblastoma. *Mol Med Rep.* 2021;24(2):1–9.
- Su Z, Chen M, Ding R, Shui L, Zhao Q, Luo W. Long noncoding RNA HCG11 suppresses the malignant phenotype of non-small cell lung cancer cells by targeting the miR875/SATB2 axis. *Mol Med Rep.* 2021;24(2):1–11.
- Liu Y, Zhou P, Wang F, Zhang X, Yang D, Hong L, Ruan D. Inhibition of lncRNA SNHG8 plays an important role in

- hypoxia-ischemia-reoxygenation-induced myocardial injury by regulating miR-335 and RASA1 expressions. *Mol Med Rep.* 2021;24(2):1–9.
16. Liu K, Chen S, Lu R. Identification of important genes related to ferroptosis and hypoxia in acute myocardial infarction based on WGCNA. *Bioengineered.* 2021;12(1):7950–63.
 17. Dietrich C, Hofmann TG. Ferroptosis meets cell–cell contacts. *Cells (Basel).* 2021;10(9):2462.
 18. Li J, Cao F, Yin HL, Huang ZJ, Lin ZT, Mao N, Sun B, Wang G. Ferroptosis: past, present, and future. *Cell Death Dis.* 2020;11(2):88.
 19. Wu C, Liu Z, Chen Z, Xu D, Chen L, Lin H, Shi J. A Nonferrous ferroptosis-like strategy for antioxidant inhibition-synergized nanocatalytic tumor therapeutics. *Sci Adv.* 2021;7(39):8833.
 20. Emmons MF, Smalley K. Ironing-out the details: new strategies for combining ferroptosis inhibitors with immunotherapy in melanoma. *J Investig Dermatol.* 2022;142(1):18–20.
 21. Liu M, Wang L, Xia X, Wu Y, Zhu C, Duan M, Wei X, Hu J, Lei L. Regulated lytic cell death in breast cancer. *Cell Biol Int.* 2022;46(1):12–33.
 22. Zhao E, Chen S, Dang Y. Development and external validation of a novel immune checkpoint-related gene signature for prediction of overall survival in hepatocellular carcinoma. *Front Mol Biosci.* 2020;7:620765.
 23. Tang Y, Li C, Zhang YJ, Wu ZH. Ferroptosis-related long non-coding RNA signature predicts the prognosis of head and neck squamous cell carcinoma. *Int J Biol Sci.* 2021;17(3):702–11.
 24. Wang Z, Jensen MA, Zenklusen JC. A practical guide to the Cancer Genome Atlas (TCGA). *Methods Mol Biol.* 2016;1418:111–41.
 25. Zhou N, Bao J. FerrDb: a manually curated resource for regulators and markers of ferroptosis and ferroptosis-disease associations. *Database (Oxford).* 2020. <https://doi.org/10.1093/database/baaa021>.
 26. Franceschini A, Szklarczyk D, Frankild S, Kuhn M, Simonovic M, Roth A, Lin J, Minguez P, Bork P, von Mering C, et al. STRING v9.1: protein–protein interaction networks, with increased coverage and integration. *Nucleic Acids Res.* 2013;41(Database issue):D808–15.
 27. Newman AM, Liu CL, Green MR, Gentles AJ, Feng W, Xu Y, Hoang CD, Diehn M, Alizadeh AA. Robust enumeration of cell subsets from tissue expression profiles. *Nat Methods.* 2015;12(5):453–7.
 28. Charoentong P, Finotello F, Angelova M, Mayer C, Efremova M, Rieder D, Hackl H, Trajanoski Z. Pan-cancer immunogenomic analyses reveal genotype-immunophenotype relationships and predictors of response to checkpoint blockade. *Cell Rep.* 2017;18(1):248–62.
 29. Yoshihara K, Shahmoradgol M, Martinez E, Vegesna R, Kim H, Torres-Garcia W, Trevino V, Shen H, Laird PW, Levine DA, et al. Inferring tumor purity, stromal, and immune cell admixture from expression data. *Nat Commun.* 2013;4:2612.
 30. Shi J, Jiang D, Yang S, Zhang X, Wang J, Liu Y, Sun Y, Lu Y, Yang K. LPAR1, correlated with immune infiltrates, is a potential prognostic biomarker in prostate cancer. *Front Oncol.* 2020;10:846.
 31. Yi M, Nissley DV, McCormick F, Stephens RM. ssGSEA score-based ras dependency indexes derived from gene expression data reveal potential ras addiction mechanisms with possible clinical implications. *Sci Rep.* 2020;10(1):10258.
 32. Li T, Fan J, Wang B, Traugh N, Chen Q, Liu JS, Li B, Liu XS. TIMER: a web server for comprehensive analysis of tumor-infiltrating immune cells. *Can Res.* 2017;77(21):e108–10.
 33. Xie YH, Chen YX, Fang JY. Comprehensive review of targeted therapy for colorectal cancer. *Signal Transduct Target Ther.* 2020;5(1):22.
 34. Yang WS, Stockwell BR. Ferroptosis death by lipid peroxidation. *Trends Cell Biol.* 2016;26(3):165–76.
 35. Friedmann AJ, Schneider M, Proneth B, Tyurina YY, Tyurin VA, Hammond VJ, Herbach N, Aichler M, Walch A, Eggenhofer E, et al. Inactivation of the ferroptosis regulator Gpx4 triggers acute renal failure in mice. *Nat Cell Biol.* 2014;16(12):1180–91.
 36. Stockwell BR, Friedmann AJ, Bayir H, Bush AI, Conrad M, Dixon SJ, Fulda S, Gascon S, Hatzios SK, Kagan VE, et al. Ferroptosis: a regulated cell death nexus linking metabolism, redox biology, and disease. *Cell.* 2017;171(2):273–85.
 37. Yang WH, Ding CC, Sun T, Rupprecht G, Lin CC, Hsu D, Chi JT. The hippo pathway effector TAZ regulates ferroptosis in renal cell carcinoma. *Cell Rep.* 2019;28(10):2501–8.
 38. Markowitsch SD, Schupp P, Lauckner J, Vakhrusheva O, Slade KS, Mager R, Efferth T, Haferkamp A, Juengel E. Artesunate inhibits growth of sunitinib-resistant renal cell carcinoma through cell cycle arrest and induction of ferroptosis. *Cancers (Basel).* 2020;12(11):3150.
 39. Lei G, Zhang Y, Hong T, Zhang X, Liu X, Mao C, Yan Y, Koppula P, Cheng W, Sood AK, et al. Ferroptosis as a mechanism to mediate p53 function in tumor radiosensitivity. *Oncogene.* 2021;40(20):3533–47.
 40. Feng X, Wang S, Sun Z, Dong H, Yu H, Huang M, Gao X. Ferroptosis enhanced diabetic renal tubular injury via HIF-1 α /HO-1 pathway in db mice. *Front Endocrinol (Lausanne).* 2021;12:626390.
 41. Sun Y, Berleth N, Wu W, Schlutermann D, Deitersen J, Stuhldreier F, Berning L, Friedrich A, Akgun S, Mendiburo MJ, et al. Fin56-induced ferroptosis is supported by autophagy-mediated GPX4 degradation and functions synergistically with mTOR inhibition to kill bladder cancer cells. *Cell Death Dis.* 2021;12(11):1028.
 42. Xiang Y, Chen X, Wang W, Zhai L, Sun X, Feng J, Duan T, Zhang M, Pan T, Yan L, et al. Natural product erianin inhibits bladder cancer cell growth by inducing ferroptosis via NRF2 inactivation. *Front Pharmacol.* 2021;12:775506.
 43. Wang R, Xing R, Su Q, Yin H, Wu D, Lv C, Yan Z. Knockdown of SFRS9 inhibits the progression of colorectal cancer through triggering ferroptosis mediated by GPX4 reduction. *Front Oncol.* 2021;11:683589.
 44. Zhong F, Liu S, Hu D, Chen L. LncRNA AC099850.3 promotes hepatocellular carcinoma proliferation and invasion through PRR11/PI3K/AKT axis and is associated with patients prognosis. *J Cancer.* 2022;13(3):1048–60.
 45. Zhou B, Guo W, Sun C, Zhang B, Zheng F. Linc00462 promotes pancreatic cancer invasiveness through the miR-665/TGFBR1-TGFBR2/SMAD2/3 pathway. *Cell Death Dis.* 2018;9(6):706.
 46. Wang L, Lin C, Sun N, Wang Q, Ding X, Sun Y. Long non-coding RNA CASC19 facilitates non-small cell lung cancer cell proliferation and metastasis by targeting the miR-301b-3p/LDLR axis. *J Gene Med.* 2020;22(12):e3254.
 47. Chen Y, Guo Y, Li S, Xu J, Wang X, Ning W, Ma L, Qu Y, Zhang M, Zhang H. Identification of N6-methyladenosine-related lncRNAs as a prognostic signature in glioma. *Front Oncol.* 2022;12:789283.
 48. Yang F, Song Y, Ge L, Zhao G, Liu C, Ma L. Long non-coding RNAs as prognostic biomarkers in papillary renal cell carcinoma. *Oncol Lett.* 2019;18(4):3691–7.
 49. Tang R, Xu J, Zhang B, Liu J, Liang C, Hua J, Meng Q, Yu X, Shi S. Ferroptosis, necroptosis, and pyroptosis in anticancer immunity. *J Hematol Oncol.* 2020;13(1):110.
 50. Song X, Long D. Nrf2 and ferroptosis: a new research direction for neurodegenerative diseases. *Front Neurosci.* 2020;14:267.
 51. Chu B, Kon N, Chen D, Li T, Liu T, Jiang L, Song S, Taviana O, Gu W. ALOX12 is required for p53-mediated tumor suppression through a distinct ferroptosis pathway. *Nat Cell Biol.* 2019;21(5):579–91.
 52. Jennis M, Kung CP, Basu S, Budina-Kolomets A, Leu JI, Khaku S, Scott JP, Cai KQ, Campbell MR, Porter DK, et al. An African-specific polymorphism in the TP53 gene impairs p53 tumor suppressor function in a mouse model. *Genes Dev.* 2016;30(8):918–930.
 53. Ou Y, Wang SJ, Li D, Chu B, Gu W. Activation of SAT1 engages polyamine metabolism with p53-mediated ferroptotic responses. *Proc Natl Acad Sci U S A.* 2016;113(44):E6806–12.
 54. Lajko E, Hegedus R, Mezo G, Kohidai L. Apoptotic effects of drug targeting conjugates containing different GnRH analogs on colon cancer cells. *Int J Mol Sci.* 2019;20(18):4421.

Publisher's Note

Springer Nature remains neutral with regard to jurisdictional claims in published maps and institutional affiliations.